

DiffDance: Cascaded Human Motion Diffusion Model for Dance Generation

Qiaosong Qi*
qiqiaosong.qqs@alibaba-inc.com
Alibaba Group
Beijing, China

Le Zhuo*
zhuole1025@gmail.com
Beihang University
Beijing, China

Aixi Zhang†
aixi.zhax@alibaba-inc.com
Alibaba Group
Beijing, China

Yue Liao
liaoyue.ai@gmail.com
Beihang University
Beijing, China

Fei Fang
mingyi.ff@alibaba-inc.com
Alibaba Group
Beijing, China

Si Liu
liusi@buaa.edu.cn
Beihang University
Beijing, China

Shuicheng Yan
shuicheng.yan@gmail.com
BAAI
Skyworks

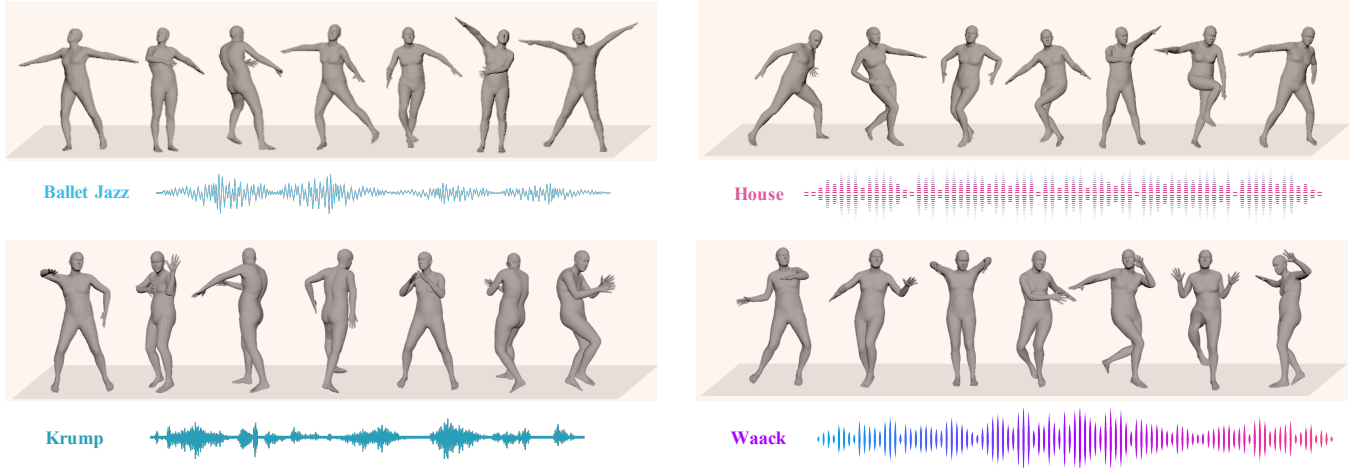


Figure 1: Dance examples generated by our DiffDance conditioned on various genres of music. Our cascaded diffusion model framework, when conditioned on aligned music representations, is capable of producing high-resolution, long-form dance sequences that correspond well with the input music.

ABSTRACT

When hearing music, it is natural for people to dance to its rhythm. Automatic dance generation, however, is a challenging task due to the physical constraints of human motion and rhythmic alignment with target music. Conventional autoregressive methods introduce

compounding errors during sampling and struggle to capture the long-term structure of dance sequences. To address these limitations, we present a novel cascaded motion diffusion model, DiffDance, designed for high-resolution, long-form dance generation. This model comprises a music-to-dance diffusion model and a sequence super-resolution diffusion model. To bridge the gap between music and motion for conditional generation, DiffDance employs a pretrained audio representation learning model to extract music embeddings and further align its embedding space to motion via contrastive loss. During training our cascaded diffusion model, we also incorporate multiple geometric losses to constrain the model outputs to be physically plausible and add a dynamic loss weight that adaptively changes over diffusion timesteps to facilitate sample diversity. Through comprehensive experiments performed on the benchmark dataset AIST++, we demonstrate that DiffDance

*Both authors contributed equally to this research.

†Corresponding author.

Permission to make digital or hard copies of part or all of this work for personal or classroom use is granted without fee provided that copies are not made or distributed for profit or commercial advantage and that copies bear this notice and the full citation on the first page. Copyrights for third-party components of this work must be honored. For all other uses, contact the owner/author(s).

MM '23, October 29–November 3, 2023, Ottawa, ON, Canada

© 2023 Copyright held by the owner/author(s).

ACM ISBN 979-8-4007-0108-5/23/10.

<https://doi.org/10.1145/3581783.3612307>

is capable of generating realistic dance sequences that align effectively with the input music. These results are comparable to those achieved by state-of-the-art autoregressive methods.

CCS CONCEPTS

• **Applied computing** → **Media arts**.

KEYWORDS

Diffusion Model, Music-to-Dance, Conditional Generation, Multimodal Learning

ACM Reference Format:

Qiaosong Qi, Le Zhuo, Aixi Zhang, Yue Liao, Fei Fang, Si Liu, and Shuicheng Yan. 2023. DiffDance: Cascaded Human Motion Diffusion Model for Dance Generation. In *Proceedings of the 31st ACM International Conference on Multimedia (MM '23)*, October 29–November 3, 2023, Ottawa, ON, Canada. ACM, New York, NY, USA, 9 pages. <https://doi.org/10.1145/3581783.3612307>

1 INTRODUCTION

See the music, hear the dance.

George Balanchine

Dance serves as a universal language that transcends not only cultural boundaries but also those between species. In recent times, dance videos have emerged as the most popular video category on social media platforms such as TikTok and YouTube. Dance is inherently intertwined with music, as individuals naturally move to the rhythm. However, creating a satisfactory dance is challenging, as it requires elegant movements that synchronize with the music on both a global style and local rhythm level, a feat that may take professional dancers years of practice. Consequently, the task of automatic dance generation from music has garnered significant interest from the deep learning community in recent years.

Existing works [14, 20, 21, 34] primarily formulate music-to-dance generation as a sequence-to-sequence generation task that autoregressively generates dance sequences. However, these approaches trained with teacher forcing strategy are susceptible to compounding error introduced by autoregressive generation, which becomes problematic for generating long sequences. Besides, conventional methods rely on handcrafted spectrogram features as music conditions, including *MFCC*, *onset strength*, *constant-Q chromagram*, etc. These features may lack a deep understanding of the music-dance relationship and could be suboptimal for music-to-dance generation.

Diffusion models, a newly developed class of non-autoregressive generative models, achieve impressive results in various tasks [5, 18, 41]. For conditional synthesis, diffusion models also demonstrate a strong capacity to generate diverse and realistic samples [27, 31]. Recent work [38] proposes Motion Diffusion Model (MDM), which achieves state-of-the-art results in text-to-motion and action-to-motion. However, we argue that directly applying existing motion diffusion models to dance generation is problematic since they are designed for motion with low temporal resolution and short sequence length. In contrast, dance sequences are usually much longer and more complex than general human motion, exhibiting global structures such as symmetrical repetitive movements. Therefore, these models struggle to model extremely long sequences and fail to produce realistic dance with long-term structure.

In this work, we aim to generate high temporal resolution dance sequences aligned with input music leveraging diffusion models. To this end, we propose a novel cascaded human diffusion model framework named DiffDance. Specifically, DiffDance is a two-stage method that contains a music-to-dance diffusion model first generating low-resolution dance sequences and a sequence super-resolution model upscaling the low-resolution sequence by filling intermediate motion between input motions. To enable conditional generation, we use Wav2CLIP [39] to map input music into learned embeddings instead of conventional handcrafted features. Models in both stages are conditioned on the learned embeddings and use classifier-free guidance [13] to improve sample quality. Since the Wav2CLIP audio encoder shares an embedding space solely with images and text, we align its embedding space to motion by freezing the motion encoder in MotionCLIP [37] and fine-tuning our audio encoder using paired data in AIST++ [21]. After fine-tuning, the audio encoder can produce latent representations aligned with motion semantics, thus further boosting music-to-dance performance. Lastly, we incorporate multiple geometric losses during training, as derived from existing motion generation literature [17, 29, 32], introducing key joints position and rotation regularization losses to prevent unnatural artifacts such as foot sliding and instant rotation. We further add a dynamic loss weight to encourage model sampling at large timesteps and correcting unnatural motion at small timesteps. As illustrated in Fig. 1, our DiffDance can generate diverse, realistic, and coherent dance sequences guided by various music inputs.

Our contributions can be summarized as follows:

- We propose a cascaded motion diffusion model that generates long-form, high-resolution dance sequences;
- We align the CLIP embedding space of music and dance for better feature representation and demonstrate the effectiveness of classifier-free guidance in music-to-dance generation;
- We incorporate a variety of geometric losses and a dynamic loss weight schedule to produce realistic samples while maintaining diversity;
- Extensive experiments demonstrate our proposed DiffDance surpasses the state-of-the-art model in terms of dance quality and music-dance correspondence.

2 RELATED WORK

2.1 Music to Dance Generation

Generating dance sequences from music, which aims to produce realistic choreographed movements aligned with input music, is a challenging task built on motion synthesis [1, 3, 6, 8]. Early works [19, 33, 44] favored the generation of 2D dance sequences from music, predominantly due to the abundant data from online dance videos. Recently, AIST++ [21], a large-scale 3D motion dataset, greatly pushed the development of 3D dance generation. Various works explore this task leveraging different network architectures, such as LSTMs [40], Transformers [14, 21, 34], and GANs [16]. Among them, works with transformer architecture achieve state-of-the-art results, highlighting the superiority of Transformers in sequence modeling. For instance, FACT [21] introduced a full-attention cross-modal transformer that generates

high-quality 3D dance sequences in an autoregressive manner. Baidando [34] designed a two-stage method consisting of pose VQ-VAE and motion GPT. The motion GPT is fine-tuned via actor-critic learning to realize temporal coherency. MNET [16] proposed a conditional GAN framework including a Transformer Generator and Discriminator to produce dance motions conditioned on multiple music genres. In contrast, our method leverages a cascaded diffusion model framework to directly generate the whole dance sequences avoiding compounding errors introduced by autoregressive generation.

It is also worth mentioning that existing methods largely overlook the aspect of music representation, typically directly using handcrafted music features extracted by Librosa [25] as conditional music features, such as *MFCC*, *onset strength*, and the *constant-Q chromagram*. However, recent advancements in text-to-image and text-to-video generation [10, 31] have demonstrated that using conditional features extracted from large-scale representation learning models can markedly enhance cross-modal generation performance. Motivated by this finding, our model deviates from traditional handcrafted music features and instead employs the Wav2CLIP [39] audio encoder, a robust audio representation learning method, for music-driven dance generation, resulting in improved dance generation performance.

2.2 Diffusion Models

Diffusion models [11, 35, 36] are a class of likelihood-based generative models that learn to recover samples from random noise via a denoising process. They have achieved great success in generating high-fidelity images [5], and demonstrate strong abilities to generalize to other domains such as audio [15] and language [22]. For conditional generation, existing models often use classifier guidance [5] or classifier-free guidance [13] to improve sample synthesis quality. Recently, some seminal works [38, 42] adapt diffusion models to motion synthesis and achieve impressive results. Specifically, MDM [38] proposed a transformer-based diffusion model that leverages classifier-free guidance to solve text-to-motion synthesis. However, dance sequences are much more difficult for diffusion models to synthesize since they have longer sequence lengths and more complex movements. In the vision domain, cascaded diffusion models [10, 12] are effective methods that can generate high-resolution samples while keeping each sub-network relatively simple. Inspired by that, we solve music-to-dance generation via a cascaded motion diffusion model. Besides, we add multiple geometric losses during training in order to ensure the model output to be physically-plausible.

3 METHOD

Our aim is to generate dance sequences $x^{1:L} = \{x^t\}_{t=1}^L$ with length L given the music condition c . For 3D dance generation, the dance sequence is represented in D -dimensional features of J body joints, resulting in a $x^t \in R^{J \times D}$ motion representation. In the following, we first briefly discuss the preliminary knowledge of diffusion models in Sec. 3.1. Then, we introduce our proposed DiffDance, a cascaded motion diffusion model trained with multiple geometric losses in Sec. 3.2. In Sec. 3.3, we finally discuss aligning music

embedding space to motion and using classifier-free guidance for music conditional generation.

3.1 Preliminaries of Diffusion Models

Diffusion models define a fixed Markovian process by gradually adding noise to sample data $x_0 \in q(x_0)$. The forward diffusion process is defined as:

$$q(x_{1:T}|x_0) := \prod_{t=1}^T q(x_t|x_{t-1}), \quad (1)$$

$$q(x_t|x_{t-1}) := \mathcal{N}(x_t; \sqrt{1 - \beta_t}x_{t-1}, \beta_t\mathbf{I}), \quad (2)$$

where $t \in [1, T]$, β_t is a pre-defined variance schedule that controls the rate of noise injection, and $q(x_t|x_{t-1})$ is a Gaussian transition kernel. After T steps, the amount of noise becomes sufficiently large, and the Markovian chain approximately converges to a standard Gaussian distribution $\mathcal{N}(0, \mathbf{I})$.

In order to convert noise back to sample for generation, diffusion models learn a reverse process via:

$$p_\theta(x_{0:T}) := p(x_T) \prod_{t=1}^T p_\theta(x_{t-1}|x_t), \quad (3)$$

$$p_\theta(x_{t-1}|x_t) := \mathcal{N}(x_{t-1}; \mu_\theta(x_t, t), \Sigma_\theta(x_t, t)), \quad (4)$$

where θ is a parameterized neural network to predict the mean of Gaussian. In practice, we simply set $\Sigma_\theta(x_t, t) = \beta_t^2\mathbf{I}$ following [11].

Diffusion models are trained by minimizing the variational upper bound on the negative log-likelihood of data. Typically, we use a simplified version with L_2 loss [11]:

$$\mathcal{L}_{simple} = \mathbb{E}_{x_0 \sim q(x_0), t \sim [1, T]} [\|\hat{\epsilon}_\theta(x_t, t) - \epsilon\|_2^2]. \quad (5)$$

Once the diffusion model is trained, we can generate a new sample x by iteratively running the reverse diffusion process from timestep T to 0.

3.2 Cascaded Motion Diffusion Model

In this section, we formulate our DiffDance, a cascaded motion diffusion model for music-to-dance generation. Fig. 2 summarizes the cascaded pipeline of our DiffDance.

Framework. DiffDance consists of a Music-to-Dance (M2D) diffusion model and a Sequence Super-Resolution (SSR) diffusion model. Specifically, the M2D model is similar to MDM [38], a transformer-based diffusion model as illustrated in Fig. 2. Different from conventional diffusion models that predict ϵ_t , our model $f_\theta^{low}(x_t, t, c)$ directly predicts the original data point x_0 , given the noised data x_t , timestep t , and music representation c . Both the timestep t and music representation c are projected into the dimension of transformer. Next, we sum these embeddings together and concatenate it with noised input x_t to guide the generation of our model.

The SSR model $f_\theta^{high}(x_t, t, c, x_{low}, s)$ aims to increase the temporal resolution of the output of our base M2D model. It shares the same architecture with the M2D model except that there is an additional low-resolution dance input x_{low} and an additional timestep s for conditioning augmentation as shown in the dotted box of Fig. 2. The SSR model first upsamples the low-resolution sequence via linearly interpolated motion frames and then channel-wise concatenates the upsampled input to the noised data x_t . We

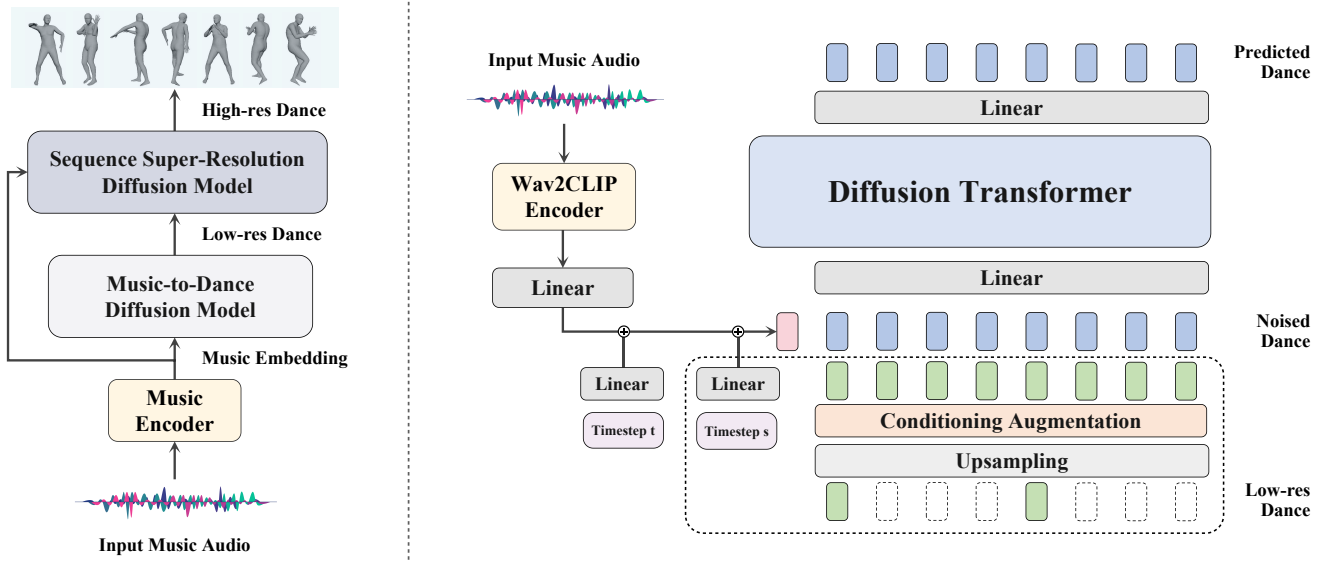


Figure 2: (Left) Overall framework. DiffDance uses a frozen music encoder to extract music features. The music-to-dance diffusion model maps music representation into a low-resolution (15-FPS) dance sequence, while the sequence super-resolution diffusion model increases its temporal resolution (60-FPS). **(Right) Model Details.** Both models receive a noised dance x_t , diffusion timestep t , and music representation c . c is extracted via Wav2CLIP encoder and then summed with t . For the sequence super-resolution model, it receives additional low-resolution dance x_{low} and timestep s , as depicted in the dotted box. After conditional augmentation, low-resolution dance is channel-wise concatenated with noised dance.

employ conditioning augmentation [12] to our SSR model. Conditioning augmentation has been proven an effective strategy to significantly improve the sample quality and model robustness in cascaded generation pipelines [12, 31]. In practice, we add Gaussian noise corresponding to a random diffusion timestep s to corrupt input motion during training. We also add s to the original diffusion timestep t as conditional information. At inference time, we sweep over all possible values of s and fix it that yields the best quality. Adding some noise to the inputs can eliminate unnatural artifacts in generated low-resolution dance sequences, thus bridging the gap between the ground-truth distribution during training and the model output distribution at inference time.

Training Objectives. Generating physically-plausible motion sequences is challenging using the original denoising objective with Equation 5. MDM adds a set of geometric losses [29, 32] to regularize the training process. These losses, denoted as L_{pos}^a , regularize the positions and position velocities of all joints equally. However, we observe undesirable motions, such as instant movements and rotations generated by our vanilla model trained with L_{pos}^a , which are unreasonable for dance choreography. To produce fluent and natural dance sequences, we further add L_{pos}^k to regularize key joints such as ‘hand’ and ‘foot’. This regularization is also from both positions and position velocities perspectives formulated as:

$$\mathcal{L}_{pos}^k = \sum_{j \in [f, h]} \|\mathbf{p}_j - \hat{\mathbf{p}}_j\|_2^2 + \|\mathbf{v}_j^p - \hat{\mathbf{v}}_j^p\|_2^2, \quad (6)$$

where f and h denote key joints of foot and hand joints respectively, and \mathcal{L}_{pos}^k constrains the difference between key joint positions $\hat{\mathbf{p}}_j$ and ground truth \mathbf{p}_j as well as position velocities $\hat{\mathbf{v}}_j^p$ and ground

truth \mathbf{v}_j^p . To account for the high complexity of motion sequences, we computed joint linear velocities with respect to the ‘root’ node’s relative velocities. Therefore, our positions’ loss function excludes the ‘root’ joint’s linear velocity.

Besides, we propose to regularize the rotations for key joints explicitly. Note that the ‘root’ joint is also regularized as a key joint for barycentric motion consistency. The rotation loss is formulated as:

$$\mathcal{L}_{rot}^k = \sum_{j \in [f, h, r]} \|\mathbf{r}_j - \hat{\mathbf{r}}_j\|_2^2 + \|\mathbf{v}_j^r - \hat{\mathbf{v}}_j^r\|_2^2, \quad (7)$$

where r denotes key joints of ‘root’, and \mathcal{L}_{rot}^k constrains the difference between key joint rotations \mathbf{r}_j and ground truth $\hat{\mathbf{r}}_j$ as well as rotation velocities \mathbf{v}_j^r and ground truth $\hat{\mathbf{v}}_j^r$.

We also find it unsuitable to apply these losses uniformly across all diffusion timesteps. As described in the analysis in [4], the backward diffusion process can be roughly divided into a generation stage and a denoising stage, corresponding to large and small timesteps, respectively. When t approaches the total timestep T , the noise becomes sufficiently large, corrupting the input dance into a noised version that has almost lost all its geometric information. Intuitively, implementing geometric losses at the generation stage will not impose physical constraints on samples but may instead impair sample quality and diversity. To address this, we introduce a simple dynamic loss decay weight $\lambda_t = 1 - \alpha \frac{t}{T}$, which linearly decreases as the diffusion timestep t increases. The overall training loss can be expressed as:

$$\mathcal{L} = \mathcal{L}_{simple} + \lambda_t (\lambda_1 \mathcal{L}_{pos}^a + \lambda_2 \mathcal{L}_{pos}^k + \lambda_3 \mathcal{L}_{rot}^k), \quad (8)$$

where λ_1, λ_2 and λ_3 are the hyper-parameter loss weights for the all joints position loss \mathcal{L}_{pos}^a , key joints position loss \mathcal{L}_{pos}^k and key joints rotation loss \mathcal{L}_{rot}^k respectively.

3.3 Conditional Generation

Given input music, our objective is to extract an effective music representation containing rich semantic information, such as the style and rhythm of the music. Subsequently, we utilize this representation as conditions to generate dance sequences aligned with the input music.

Music Representations. Previous approaches have not placed significant emphasis on music representations for conditional generation. These methods primarily employ handcrafted music features, e.g., *onset strength* as rhythmic features, and *constant-Q chromagram* as chroma features. One distinct drawback of these features is that they lack high-level semantics critical to cross-modality generation. CLIP [30], a large-scale visual-textual embedding model, has demonstrated its efficacy for text-guided generation works [10, 31]. Likewise, we propose to use the audio encoder of Wav2CLIP [39], which encodes an audio clip into a 512-dimensional vector that shares an embedding space with text and image in CLIP. However, there still exists a significant domain gap between extracted music representations and dance motions since the Wav2CLIP audio encoder is solely trained on general audio-visual datasets. To better align the embedding space of music audio with dance motions, we fine-tune our audio encoder by adding multi-layer perceptrons as adapter layers and map its output to a motion encoder, as illustrated in Fig. 3.

Specifically, we use the motion encoder in [37], which also extracts a 512-dimensional embedding aligned with CLIP joint representation. To mitigate modal collapse, we freeze the weights of both the motion encoder and music encoder during fine-tuning and only train the adapter layers with InfoNCE loss [2]. The music-to-dance contrastive loss for the i -th pair between music clip m_i and dance sequence d_i is formulated as:

$$\mathcal{L}_i^{m \rightarrow d} = -\log \frac{\exp [s(m_i, d_i) / \tau]}{\sum_{j=1}^N \exp [s(m_i, d_j) / \tau]}, \quad (9)$$

where $s(m_i, d_i)$ represents the cosine similarity, and τ is a learnable temperature parameter.

Classifier-free Guidance. After learning the music-dance joint embedding space, we extract music representations and leverage classifier-free guidance [13] to improve sample quality. In practice, we jointly train a single diffusion model on both conditional and unconditional objectives by randomly dropping the music condition c . During sampling, we can improve sample quality by adjusting the x_0 prediction using:

$$f_{\theta}(x_t, t, c) = w f_{\theta}(x_t, t, c) + (1 - w) f_{\theta}(x_t, t, \emptyset), \quad (10)$$

where $f_{\theta}(x_t, t, c)$ and $f_{\theta}(x_t, t, \emptyset)$ correspond to the conditional and unconditional model respectively, and w is the guidance strength which is typically set greater than 1 to enable classifier-free guidance. We apply classifier-free guidance for both models in the two-stage pipeline.

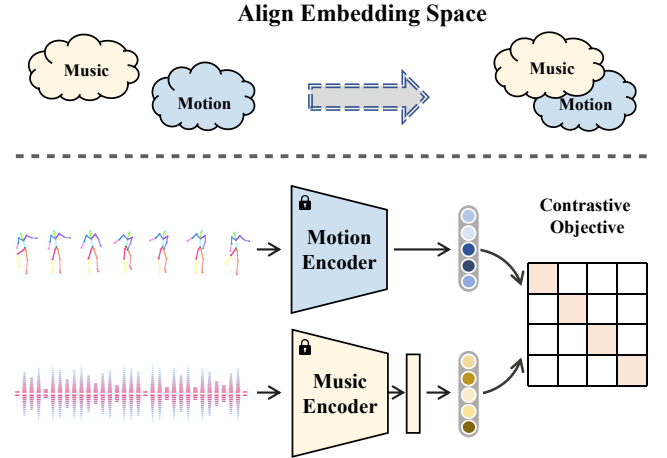


Figure 3: Alignment of music and motion. We introduce adapter layers to the music encoder and employ a contrastive loss to align the embedding spaces of music and motion.

4 EXPERIMENTS

4.1 Dataset

AIST++ [21] is a large-scale publicly available 3D human dance dataset containing 1363 3D dance sequences and music pairs. There are 980 training sets, 40 test sets, and 343 candidate sets in AIST++. Note that the candidate sets are not recommended by AIST++ for training or evaluation. In terms of data format, dance motion is represented as 60-FPS 3D pose sequences in SMPL format [23]. We conduct all the experiments on the AIST++ dataset and follow the experimental setting in [34].

4.2 Implementation Details

Alignment Setting. For fine-tuning the Wav2CLIP adapter which consists of 2 MLP layers with 512 hidden size, we use AdamW [24] with learning-rate $1e^{-5}$ and train 100 epochs with batch size 64. Music is loaded by Librosa [25] and split into multiple clips of 6 seconds. Dance sequences are represented in rotation 6d format [43] and also split into 6-second clips correspondingly. Similar to the experimental setting in MotionCLIP [37], we down-sample the frame rate of dance clips from 60-FPS to 30-FPS.

Cascaded Diffusion Model Setting. We train our cascaded diffusion model for 500 epochs using AdamW with learning-rate $1e^{-4}$. Music is loaded by Librosa and split into 20-second clips, and the dance sequences are split correspondingly with rotation 6d representation. Music is mapped to 512-dim vectors via frozen Wav2CLIP-adapter. For classifier-free guidance, we randomly mask 10% music condition c at each training step. The diffusion transformer has 12 layers with 768-dim hidden size and 6 heads. The dropout ratio is set to 0.1. All the geometric losses weights λ_1, λ_2 , and λ_3 are set to 1.0, and the decay coefficient α for λ_t is set to 0.1. For the base M2D model at the first stage, we set batch size to 32. We use dance sequences of 20 seconds to learn the long-term dance semantics and down-sample FPS from 60 to 15. For the SSR model at the second stage, we set batch size 8, and keep FPS for high-resolution

Method	Motion Quality		Motion Diversity		Beat Align Score \uparrow	User Study
	FID $_k$ \downarrow	FID $_g$ \downarrow	Div $_k$ \uparrow	Div $_g$ \uparrow		Our Method Wins
Ground Truth	17.10	10.60	8.19	7.45	0.2374	44.8%
Li <i>et al.</i> [7]	86.43	43.46	6.85*	3.32	0.1607	98.0%
DanceNet [44]	69.18	25.49	2.86	2.85	0.1430	92.0%
DanceRevolution [14]	73.42	25.92	3.52	4.87	0.1950	90.8%
FACT [21]	35.35	22.11	5.94	<u>6.18</u>	0.2209	96.8%
Bailando [34]	<u>28.16</u>	9.62	7.83	6.34	<u>0.2332</u>	74.4%
DiffDance (Ours)	24.09	<u>20.68</u>	<u>6.02</u>	2.89	0.2418	-

Table 1: Baselines comparison on AIST++. Best values are in bold, and runner-up values are underlined. Quantitatively, our model achieves state-of-the-art performance on FID $_k$ and Beat Align Score. Qualitatively, our model generates more realistic dance sequences and outperforms baseline approaches in the user study. \downarrow indicates lower is better, and \uparrow indicates higher is better. *Note that Li *et al.* generates discontinuous and jittery motion, leading to abnormally high Div $_k$, which is also reported in [21, 34].

dance sequences to the default value of 60. The whole cascaded framework trains on 4 Tesla V100 GPUs in 24 hours.

In the inference stage, we generate a 20-second (1200 frames) dance sequence, guided by a 2-second (120 frames) seed dance sequence, and set the classifier-free guidance weight w to 2.5. We set the inference diffusion timestep T to 100, as we observe no significant difference between samples generated using the original timesteps and the reduced timesteps of 100s.

4.3 Evaluation Metrics

We follow previous works [21, 34] to quantitatively evaluate the generated samples in terms of dance quality, dance diversity, and music beat alignment. To evaluate dance quality, we first extract kinetic features [28] and geometric features [26] of ground truth and generated samples. Then we calculate Fréchet Inception Distance (FID) [9] score, including FID $_k$ based on kinetic features and FID $_g$ based on geometric features. For dance diversity, we calculate the average feature distance of kinetic features and geometric features following [21], denoted as Div $_k$ and Div $_g$, respectively. As for dance-music consistency, we use Beat Alignment Score (BAS) introduced in [21], which calculates the average distance between music beat and its nearest dance beat:

$$\text{BAS} = \frac{1}{m} \sum_{i=1}^m \exp \left(- \frac{\min_{b_j^d \in B^d} \| b_i^d - b_j^m \|^2}{2\sigma^2} \right), \quad (11)$$

where $B^d = \{b_i^d\}$ is the dance beats defined as the local minima of the kinetic velocity, $B^m = \{b_i^m\}$ is the music beats extracted using Librosa [25] toolbox, and σ is a normalized parameter which is set to 3 in all the experiments.

4.4 Comparison with Baselines

We mainly compare our proposed DiffDance with several existing methods, including Li *et al.* [20], DanceNet [44], DanceRevolution [14], FACT [21] and current state-of-the-art method Bailando [34]. Following [34], we generate 40 dance sequences for 20-second music clips in AIST++ test set and calculate the evaluation metrics. According to the comparisons shown in Table 1, our proposed DiffDance demonstrates comparable generative ability with state-of-the-art approaches, achieving 2 best and 2 runner-up in all 5 objective evaluation metrics. Moreover, more users prefer

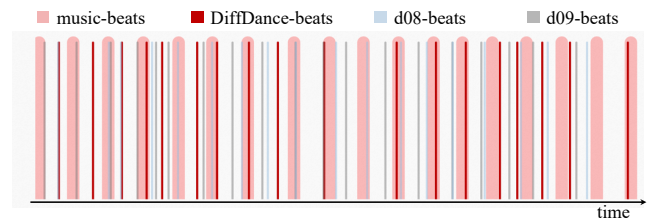


Figure 4: Beats alignment visualization. We present a visualization of music beats, kinematic beats of generated dances, and two ground truth dances. The distances between generated beats and music beats are smaller, indicating better rhythmic alignment.

our generated dance sequences compared to other methods in the user study.

Motion Quality. As shown in Table 1, our DiffDance achieves FID $_k$ score of 24.09 and FID $_g$ score of 20.68. Compared with existing methods, our model achieves the best FID $_k$, which outperforms 14.45% with a margin of 4.07 than the state-of-the-art method Bailando. This indicates that the kinetic features of generated samples, which guarantee dance characteristics, including motion velocities and energies, are much closer to those of ground truth dance distribution. As for the FID $_g$ score, which reflects the quality of choreography units, we achieve the second-best performance, which is 6.47% better than FACT with a margin of 1.43.

We investigated the reasons that the FID $_g$ score of Bailando is much better than other methods, including ours. Firstly, Bailando adopts a Choreographic Memory Codebook to record and quantize dancing units from the 980 dances of the AIST++ training set, which remembers the inherent dancing units of AIST++ to a certain extent. Secondly, all 1363 dances in AIST++ dataset are used during evaluation (the train/test split is based on music-dance pairs). As a result, more than 70% ground truth dancing units of the evaluation set have been memorized and quantized during training. The above two aspects will result in an overestimation of the FID $_g$ score, which is affected by the distance of geometric features between generated dance sequences and ground truth. As reported in Bailando, the quantization of dancing positions is essential, which helps FID $_g$

Method	FID _k ↓	Div _k ↑	BAS↑
Ground Truth	17.10	8.19	0.2374
DiffDance	24.09	6.02	0.2418
w/o two stage	29.55	5.98	0.2319
w/o align CLIP	33.78	4.37	0.2191
w/o classifier-free	30.38	4.67	0.2359
w/o loss decay	29.71	5.06	0.2257

Table 2: Ablation study of model architectures. We compare the performance of full DiffDance and several architecture variants.

score improve from 147.28 to 9.2 with a considerable margin. Therefore, we argue that Bailando overestimates FID_g evaluation. Our DiffDance is comparatively more general, as our model does not directly memorize dance units in the dataset, and the FID_g score of DiffDance still outperforms other methods except Bailando.

Motion Diversity. Motion diversity is represented as the average Euclidean distance of generated dances in the kinetic and geometric feature spaces. Table 1 shows that our DiffDance achieves Div_k of 6.02 and Div_g of 2.89. The diversity of geometric features underperforms several previous methods partly due to the introduction of multiple regularization losses, which might limit the solution space of generated dance even with a dynamic loss weight. Besides, the guidance strength w used in classifier-free guidance also has a trade-off between sample quality and diversity. For $w > 1$, this over-emphasizes the importance of condition c during sampling, which might lead to higher quality but less diverse samples.

Beat Align Score. It is important for dance generation approaches to produce dance sequences that align well with input music. Our DiffDance achieves the best beat align score of 0.2418, which outperforms 3.69% over Bailando. We even obtain a better beat align score than ground truth (0.2418 v.s. 0.2374). As shown in Fig. 4, the distance between music beats and dance beats of our DiffDance is smaller than ground-truth beats. This reflects that our model can generate dance sequences that tightly follow the beats of music, and has a deep understanding of music semantics corresponding to dance movements, indicating the effectiveness of aligning the Wav2CLIP music embedding space to motion and the use of classifier-free guidance.

However, it is crucial to note that this does not necessarily imply that DiffDance surpasses human performances in every aspect of dance. The BAS strictly rewards dance beats synchronized with music beats, yet a precise one-to-one mapping between the two doesn’t invariably exist. Human performances may excel in other aspects of dance, such as expressiveness, creativity, and emotion, without necessarily maintaining a perfect alignment with the musical beat. This observation suggests that a new metric is needed in the future for further assessment of rhythmic alignment between music and dance.

User Study. Compared with objective evaluations for dance generation, subjective evaluation can provide a comprehensive performance comparison. Therefore, we conduct extensive user studies where we ask the participants to choose their preferred dance sequence generated by each previous method (including ground truth)

Method	FID _k ↓	Div _k ↑	BAS↑
MDM-base	54.35	3.32	0.2266
+ position	41.55	3.87	0.2631
+ position velocity	24.87	5.55	0.2412
+ rotation	35.88	6.89	0.2257
+ rotation velocity	28.50	5.41	0.2636
+ ALL	19.47	7.09	0.2384

Table 3: Ablation study of loss functions. We compare the performance of our base music-to-dance model trained with different losses.

Method	FID _k ↓	Div _k ↑	BAS↑
Ground Truth	17.10	8.19	0.2374
$s = 0$	24.67	5.88	0.2145
$s = 10$	24.35	5.81	0.2223
$s = 20$	24.38	5.88	0.2309
$s = 30$	24.09	6.02	0.2418
$s = 40$	24.57	5.80	0.2327

Table 4: Ablation study of conditioning augmentation. We compare various diffusion timesteps s used in the SSR model during sampling. $s = 0$ represents the model without conditioning augmentation.

and our DiffDance. Specifically, we invite 30 participants with diverse demographic backgrounds, including 10 experts with expert knowledge in dance choreography and 20 non-experts. Using the AIST++ test set, we randomly crop 100 music clips of 20 seconds and generate 100 music-dance pairs for each method, resulting in 700 pairs in total. For each compared method, each participant is randomly assigned 10 dance sequences together with corresponding dance sequences generated by our DiffDance with the same input music. We ask the participant to indicate the preferred one by “*Considering the music genres, rhythm, motion harmony, and diversity, which dance sequence overall is better aligned with the music*” in every two candidates. Table 1 shows the statistic results, where our DiffDance outperforms all other methods with at least 74.4% winning rate. It is noteworthy that many participants find that dance sequences generated by our method usually have distinct long-term choreographic structures, such as repeating the same action in different directions.

4.5 Ablation Studies

Model Architecture. We explore the effectiveness of the following 4 architecture settings as shown in Table 2. a) Two-stage pipeline. Compared to the one-stage model as ‘w/o two-stage’, DiffDance improves FID_k by 5.46 (22.67%), which reflects that the cascaded framework is essential for high-resolution dance generation. We also present the qualitative results of both stages to demonstrate how our cascaded framework enhances the overall performance of dance generation. As depicted in Fig. 5, we visualize three distinct functions of the SSR model. First, the SSR model can increase the temporal resolution by generating meaningful dance frames as interpolations, which is its primary function. Second, the SSR model can create new relative motion inspired by low-resolution dance

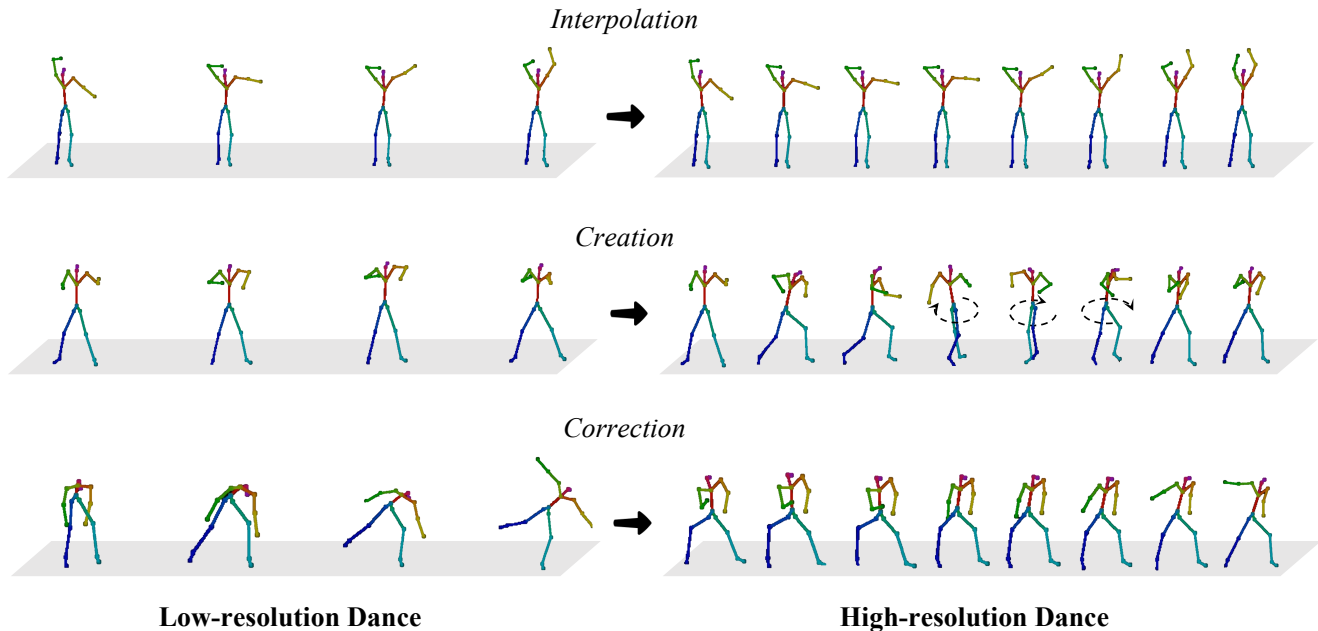


Figure 5: Visualization of outputs from both stages of our cascaded model. The base M2D model generates low-resolution dance sequences containing key motions. The SSR model improves low-resolution outputs by interpolating dance frames for increased temporal resolution, producing novel and meaningful relative dance frames, and rectifying ataxic poses. This highlights the advantages of our two-stage configuration.

frames, improving the motion diversity of DiffDance. Third, the SSR model can further correct unreasonable and uncoordinated motion frames generated by the low-resolution model, enhancing the robustness of DiffDance. By integrating these functions, our cascaded framework is able to generate realistic dance movements.

b) Alignment of music and motion embedding spaces. Compared to ‘w/o align CLIP’, DiffDance improves FID_k by 9.69 (40.22%). This indicates the effectiveness of aligning music and motion embedding spaces for better semantic music representation before training DiffDance. c) Classifier-free guidance. Compared to ‘w/o classifier-free’, DiffDance improves FID_k by 6.29 (26.11%). d) Dynamic loss decay weight. Compared to ‘w/o loss decay’, DiffDance improves FID_k by 5.62 (23.33%).

Loss Function. We conduct loss-setting experiments on the first stage base M2D model and evaluate the model on the low-resolution ground truths for efficient comparisons. The results for the whole cascaded pipeline can be extended similarly. We demonstrate the results in Table 3. For only using losses in MDM [38] denoted as ‘MDM-base’, FID_k is only 54.35, and fluctuates dramatically during the whole training process, producing highly jittery dance sequences. With regularizing the key joints in Equation 6 and 7 and adding ‘position’, ‘position velocity’, ‘rotation’ and ‘rotation velocity’ losses separately, FID_k improves to 41.55, 24.87, 35.88 and 28.50 respectively. Finally, by adding all these geometric losses, we achieve the best FID_k of 19.47.

Conditioning Augmentation. For conditioning augmentation, we compare various diffusion timestep s to corrupt dance generated by the base M2D model as input condition of the SSR model. We

show the results in Table 4, where we sweep the timestep s from 0 to 40. Note that $s = 0$ means no conditioning augmentation is used for training and testing. Our model achieves the best quality and diversity at $s = 30$, which is 30% of the SSR diffusion timestep T . This indicates that adding moderate amounts of noise augmentation is beneficial for the cascaded generation pipeline. We fixed this noise ratio during sampling for all other experiments.

5 CONCLUSION

In this paper, we introduce a cascaded motion diffusion framework called DiffDance for music-driven dance generation. DiffDance comprises a base music-to-dance diffusion model and a sequence super-resolution diffusion model capable of generating high-resolution, long-form dance sequences with temporal consistency. To enhance semantic music representation, we align the music embedding space with motion by fine-tuning our music encoder using a contrastive objective. Additionally, we employ classifier-free guidance in the music-to-dance diffusion process. We also incorporate various geometric losses and a dynamic loss decay weight to improve the fidelity and diversity of dance samples. Comprehensive experimental results demonstrate the superiority of our method from both qualitative and quantitative perspectives.

ACKNOWLEDGEMENT

This work was supported in part by the National Key R&D Program of China under Grant 2022ZD0115502, the National Natural Science Foundation of China under Grant 62122010, and the CCF-DiDi GAIA Collaborative Research Funds for Young Scholars.

REFERENCES

- [1] Emre Aksan, Manuel Kaufmann, and Otmar Hilliges. 2019. Structured prediction helps 3d human motion modelling. In *Proceedings of the IEEE/CVF International Conference on Computer Vision*. 7144–7153.
- [2] Jean-Baptiste Alayrac, Adrià Recasens, Rosalia Schneider, Relja Arandjelović, Jason Ramapuram, Jeffrey De Fauw, Lucas Smaira, Sander Dieleman, and Andrew Zisserman. 2020. Self-Supervised MultiModal Versatile Networks. In *NeurIPS*.
- [3] Judith Butepage, Michael J Black, Danica Kragic, and Hedvig Kjellstrom. 2017. Deep representation learning for human motion prediction and classification. In *Proceedings of the IEEE conference on computer vision and pattern recognition*. 6158–6166.
- [4] Kamil Deja, Anna Kuzina, Tomasz Trzcinski, and Jakub M Tomczak. 2022. On Analyzing Generative and Denoising Capabilities of Diffusion-based Deep Generative Models. In *Advances in Neural Information Processing Systems*.
- [5] Prafulla Dhariwal and Alexander Nichol. 2021. Diffusion models beat gans on image synthesis. *Advances in Neural Information Processing Systems* 34 (2021), 8780–8794.
- [6] Yinglin Duan, Tianyang Shi, Zhipeng Hu, Zhengxia Zou, Changjie Fan, Yi Yuan, and Xi Li. 2021. Automatic Translation of Music-to-Dance for In-Game Characters. In *IJCAI*.
- [7] Joao P Ferreira, Thiago M Coutinho, Thiago L Gomes, José F Neto, Rafael Azevedo, Renato Martins, and Erickson R Nascimento. 2021. Learning to dance: A graph convolutional adversarial network to generate realistic dance motions from audio. *Computers & Graphics* 94 (2021), 11–21.
- [8] Alejandro Hernandez, Jurgen Gall, and Francesc Moreno-Noguer. 2019. Human motion prediction via spatio-temporal inpainting. In *Proceedings of the IEEE/CVF International Conference on Computer Vision*. 7134–7143.
- [9] Martin Heusel, Hubert Ramsauer, Thomas Unterthiner, Bernhard Nessler, and Sepp Hochreiter. 2017. Gans trained by a two time-scale update rule converge to a local nash equilibrium. *Advances in neural information processing systems* 30 (2017).
- [10] Jonathan Ho, William Chan, Chitwan Saharia, Jay Whang, Ruiqi Gao, Alexey Gritsenko, Diederik P Kingma, Ben Poole, Mohammad Norouzi, David J Fleet, et al. 2022. Imagen video: High definition video generation with diffusion models. *arXiv preprint arXiv:2210.02303* (2022).
- [11] Jonathan Ho, Ajay Jain, and Pieter Abbeel. 2020. Denoising diffusion probabilistic models. *Advances in Neural Information Processing Systems* 33 (2020), 6840–6851.
- [12] Jonathan Ho, Chitwan Saharia, William Chan, David J Fleet, Mohammad Norouzi, and Tim Salimans. 2022. Cascaded Diffusion Models for High Fidelity Image Generation. *J. Mach. Learn. Res.* 23 (2022), 47–1.
- [13] Jonathan Ho and Tim Salimans. 2021. Classifier-Free Diffusion Guidance. In *NeurIPS Workshop on Deep Generative Models and Downstream Applications*.
- [14] Ruozhi Huang, Huang Hu, Wei Wu, Kei Sawada, Mi Zhang, and Daxin Jiang. 2021. Dance Revolution: Long-Term Dance Generation with Music via Curriculum Learning. In *ICLR*.
- [15] Rongjie Huang, Max WY Lam, Jun Wang, Dan Su, Dong Yu, Yi Ren, and Zhou Zhao. 2022. FastDiff: A Fast Conditional Diffusion Model for High-Quality Speech Synthesis. In *IJCAI*.
- [16] Jinwoo Kim, Heeseok Oh, Seongjean Kim, Hoseok Tong, and Sanghoon Lee. 2022. A Brand New Dance Partner: Music-Conditioned Pluralistic Dancing Controlled by Multiple Dance Genres. In *Proceedings of the IEEE/CVF Conference on Computer Vision and Pattern Recognition*. 3490–3500.
- [17] Muhammed Kocabas, Nikos Athanasiou, and Michael J Black. 2020. Vibe: Video inference for human body pose and shape estimation. In *Proceedings of the IEEE/CVF conference on computer vision and pattern recognition*. 5253–5263.
- [18] Zhifeng Kong, Wei Ping, Jiayi Huang, Kexin Zhao, and Bryan Catanzaro. 2021. DiffWave: A Versatile Diffusion Model for Audio Synthesis. In *ICLR*.
- [19] Juheon Lee, Seohyun Kim, and Kyogu Lee. 2018. Listen to dance: Music-driven choreography generation using autoregressive encoder-decoder network. *arXiv preprint arXiv:1811.00818* (2018).
- [20] Jiaman Li, Yihang Yin, Hang Chu, Yi Zhou, Tingwu Wang, Sanja Fidler, and Hao Li. 2020. Learning to Generate Diverse Dance Motions with Transformer. *ArXiv abs/2008.08171* (2020).
- [21] Ruilong Li, Shan Yang, D A Ross, and Angjoo Kanazawa. 2021. AI choreographer: Music conditioned 3d dance generation with aist++. In *ICCV*.
- [22] Xiang Lisa Li, John Thickstun, Ishaan Gulrajani, Percy Liang, and Tatsunori B Hashimoto. 2022. Diffusion-LM Improves Controllable Text Generation. (2022).
- [23] Matthew Loper, Naureen Mahmood, Javier Romero, Gerard Pons-Moll, and Michael J. Black. 2015. SMPL: A Skinned Multi-Person Linear Model. *SIGGRAPH Asia* 34, 6 (Oct. 2015), 248:1–248:16.
- [24] Ilya Loshchilov and Frank Hutter. 2017. Decoupled weight decay regularization. *arXiv preprint arXiv:1711.05101* (2017).
- [25] Brian McFee, Colin Raffel, Dawen Liang, Daniel PW Ellis, Matt McVicar, Eric Battenberg, and Oriol Nieto. 2015. librosa: Audio and music signal analysis in python. In *SciPy*.
- [26] Meinard Müller, Tido Röder, and Michael Clausen. 2005. Efficient content-based retrieval of motion capture data. In *SIGGRAPH*. 677–685.
- [27] Alex Nichol, Prafulla Dhariwal, Aditya Ramesh, Pranav Shyam, Pamela Mishkin, Bob McGrew, Ilya Sutskever, and Mark Chen. 2021. GLIDE: Towards Photo-realistic Image Generation and Editing with Text-Guided Diffusion Models. *arXiv:2112.10741* (2021).
- [28] Kensuke Onuma, Christos Faloutsos, and Jessica K Hodgins. 2008. FMDistance: A Fast and Effective Distance Function for Motion Capture Data.. In *Eurographics*. 83–86.
- [29] Mathis Petrovich, Michael J Black, and Gül Varol. 2021. Action-conditioned 3d human motion synthesis with transformer vae. In *Proceedings of the IEEE/CVF International Conference on Computer Vision*. 10985–10995.
- [30] Alec Radford, Jong Wook Kim, Chris Hallacy, Aditya Ramesh, Gabriel Goh, Sandhini Agarwal, Girish Sastry, Amanda Askell, Pamela Mishkin, Jack Clark, et al. 2021. Learning transferable visual models from natural language supervision. In *International Conference on Machine Learning*. PMLR, 8748–8763.
- [31] Chitwan Saharia, William Chan, Saurabh Saxena, Lala Li, Jay Whang, Emily Denton, Seyed Kamyar Seyed Ghasemipour, Burcu Karagol Ayan, S Sara Mahdavi, Rapha Gontijo Lopes, et al. 2022. Photorealistic Text-to-Image Diffusion Models with Deep Language Understanding. *arXiv preprint arXiv:2205.11487* (2022).
- [32] Mingyi Shi, Kfir Aberman, Andreas Aristidou, Taku Komura, Dani Lischinski, Daniel Cohen-Or, and Baoquan Chen. 2020. Motionet: 3d human motion reconstruction from monocular video with skeleton consistency. *ACM Transactions on Graphics (TOG)* 40, 1 (2020), 1–15.
- [33] Eli Shlizerman, Lucio Dery, Hayden Schoen, and Ira Kemelmacher-Shlizerman. 2018. Audio to body dynamics. In *Proceedings of the IEEE conference on computer vision and pattern recognition*. 7574–7583.
- [34] Li Siyao, Weijiang Yu, Tianpei Gu, Chunze Lin, Quan Wang, Chen Qian, Chen Change Loy, and Ziwei Liu. 2022. Bailando: 3D dance generation via Actor-Critic GPT with Choreographic Memory. In *CVPR*.
- [35] Jascha Sohl-Dickstein, Eric Weiss, Niru Maheswaranathan, and Surya Ganguli. 2015. Deep unsupervised learning using nonequilibrium thermodynamics. In *International Conference on Machine Learning*. PMLR, 2256–2265.
- [36] Yang Song and Stefano Ermon. 2019. Generative modeling by estimating gradients of the data distribution. *Advances in Neural Information Processing Systems* 32 (2019).
- [37] Guy Tevet, Brian Gordon, Amir Hertz, Amit H Bermano, and Daniel Cohen-Or. 2022. MotionCLIP: Exposing Human Motion Generation to CLIP Space. *arXiv preprint arXiv:2203.08063* (2022).
- [38] Guy Tevet, Sigal Raab, Brian Gordon, Yonatan Shafir, Amit H Bermano, and Daniel Cohen-Or. 2022. Human Motion Diffusion Model. *arXiv preprint arXiv:2209.14916* (2022).
- [39] Ho-Hsiang Wu, Prem Seetharaman, Kundan Kumar, and Juan Pablo Bello. 2022. Wav2clip: Learning robust audio representations from clip. In *ICASSP 2022-2022 IEEE International Conference on Acoustics, Speech and Signal Processing (ICASSP)*. IEEE, 4563–4567.
- [40] Nelson Yalta, Shinji Watanabe, Kazuhiro Nakadai, and Tetsuya Ogata. 2019. Weakly-supervised deep recurrent neural networks for basic dance step generation. In *2019 International Joint Conference on Neural Networks (IJCNN)*. IEEE, 1–8.
- [41] Xiaohui Zeng, Arash Vahdat, Francis Williams, Zan Gojic, Or Litany, Sanja Fidler, and Karsten Kreis. 2022. LION: Latent Point Diffusion Models for 3D Shape Generation. In *Advances in Neural Information Processing Systems*.
- [42] Mingyuan Zhang, Zhongang Cai, Liang Pan, Fangzhou Hong, Xinying Guo, Lei Yang, and Ziwei Liu. 2022. Motiondiffuse: Text-driven human motion generation with diffusion model. *arXiv preprint arXiv:2208.15001* (2022).
- [43] Yi Zhou, Connolly Barnes, Jingwan Lu, Jimei Yang, and Hao Li. 2019. On the continuity of rotation representations in neural networks. In *Proceedings of the IEEE/CVF Conference on Computer Vision and Pattern Recognition*. 5745–5753.
- [44] Wenlin Zhuang, Congyi Wang, Si-Yu Xia, Jinxiang Chai, and Yangang Wang. 2020. Music2Dance: DanceNet for Music-driven Dance Generation. *arXiv: Computer Vision and Pattern Recognition* (2020).